

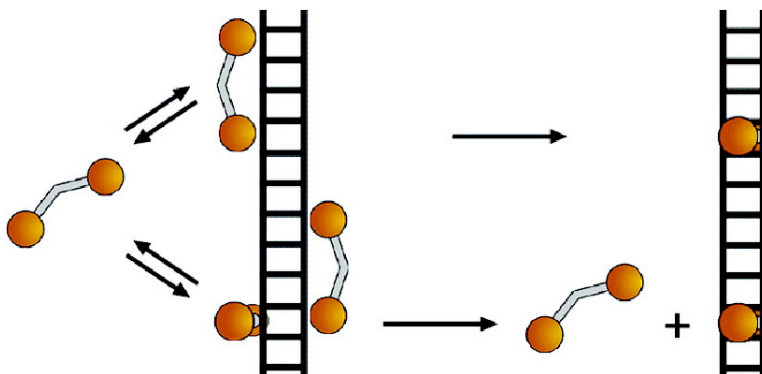
Communication

**Mechanism of DNA Threading Intercalation of Binuclear Ru Complexes: Uni- or Bimolecular Pathways Depending on Ligand Structure and Binding Density**

Pr Nordell, and Per Lincoln

*J. Am. Chem. Soc.*, **2005**, 127 (27), 9670-9671 • DOI: 10.1021/ja0521674 • Publication Date (Web): 15 June 2005

Downloaded from <http://pubs.acs.org> on March 25, 2009



**More About This Article**

Additional resources and features associated with this article are available within the HTML version:

- Supporting Information
- Links to the 10 articles that cite this article, as of the time of this article download
- Access to high resolution figures
- Links to articles and content related to this article
- Copyright permission to reproduce figures and/or text from this article

[View the Full Text HTML](#)

## Mechanism of DNA Threading Intercalation of Binuclear Ru Complexes: Uni- or Bimolecular Pathways Depending on Ligand Structure and Binding Density

Pär Nordell and Per Lincoln\*

Department of Chemistry and Bioscience, Chalmers University of Technology, SE-41296 Gothenburg, Sweden

Received April 5, 2005; E-mail: lincoln@chalmers.se

The DNA binding properties of substitution-inert transition-metal complexes have lately captured an extensive interest. A number of applications are discussed, several involving the design of complexes of recognizing ability to be used as conformational probes or in selective chemotherapy.<sup>1</sup> Due to the strong, distinct binding and bright luminescence upon intercalation of double helical DNA, ruthenium(II) complexes containing a dipyrindophenazine (dppz) ligand are interesting in this context.<sup>2</sup> Through development of binuclear complexes, such as the semirigid  $\Delta, \Delta$ - $[\mu$ -(11,11'-bidppz)-(phen)<sub>4</sub>Ru<sub>2</sub>]<sup>4+</sup> ( $\Delta, \Delta$ -**P**<sub>4</sub>, Figure 1), improved chiral discrimination has been obtained, combined with exceptionally slow intercalation kinetics.<sup>3</sup> Since binding involves threading of one of the bulky ruthenium centers through the base stack, it requires large transient conformational changes of the DNA helix. The high level of structural discrimination, accordingly attained from linking two monointercalators, makes binuclear ruthenium complexes interesting candidates as selective DNA targeting agents.

Initially, the semirigid complexes bind with high affinity on the outside of the DNA in a nonluminescent binding mode, indicated by linear dichroism to be semi-intercalation for the  $\Lambda, \Lambda$ -enantiomers.<sup>3</sup> The complexes become luminescent when threading through the DNA, where upon one dppz moiety is fully intercalated. To widen the mechanistic understanding of the threading process, we have investigated the kinetic effects of complex structure and DNA sequence. Since the rearrangement kinetics, in general, is found to be multiphasic,<sup>3b,c,4</sup> it was quite a surprise when we found a system that obeyed a very simple rate law:  $\Lambda, \Lambda$ -**B**<sub>4</sub> binding to poly(dA-dT)<sub>2</sub>, as measured by luminescence, is well described by a single exponential at a [basepair]/[complex] ratio of 8.<sup>5</sup> More intriguing was the finding that, under the same conditions, the closely related complex  $\Lambda, \Lambda$ -**P**<sub>4</sub> follows a second-order rate law, rate =  $k \times [\text{nonthreaded complex}]^2$  (Figure 2). These observations suggest that multiple pathways indeed exist for threading through the DNA, and that the choice of pathway is sensitive to small structural changes of the complex.

The study was extended by measurements at larger [basepair]/[complex] ratios (16, 32, and 64), which showed that the kinetics of threading of  $\Lambda, \Lambda$ -**B**<sub>4</sub> is practically independent of binding density (Figure S1, Supporting Information), agreeing with the reaction being of first-order nature. In sharp contrast to the **B**<sub>4</sub> complex, binding of the **P**<sub>4</sub> analogue was found to go to completion faster at larger [basepair]/[complex] ratios, and furthermore showing gradual transition to a clean pseudo-first-order kinetics at a ratio of 64 (Figure 3). Thus, while the threading of  $\Lambda, \Lambda$ -**B**<sub>4</sub> can be described as a unimolecular rearrangement of an initially bound state, the behavior of  $\Lambda, \Lambda$ -**P**<sub>4</sub> rather suggests a bimolecular rate law of the form, rate =  $k \times [\text{nonthreaded binding sites}] \times [\text{nonthreaded complex}]$ . However, such a simple model did not produce a satisfactory fit to the experimental data, which is not surprising since it does not differentiate between free binding sites and binding sites occupied by the initially bound nonthreaded complexes.

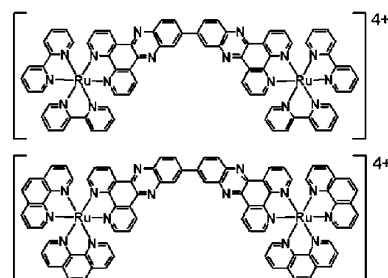


**Figure 1.** Structures of the semirigid binuclear ruthenium complexes of the current work:  $[\mu$ -(11,11'-bidppz)<sub>X</sub>Ru<sub>2</sub>]<sup>4+</sup>, X = 2,2'-bipyridine (**B**, top) and X = 1,10'-phenanthroline (**P**, bottom), 11,11'-bidppz = 11,11'-bis-(dipyrido[3,2-*a*:2',3'-*c*]phenaziny). The octahedral coordination of the Ru centers gives rise to two stereoisomeric forms: the right-handed ( $\Delta$ ) and the left-handed ( $\Lambda$ ) propeller.

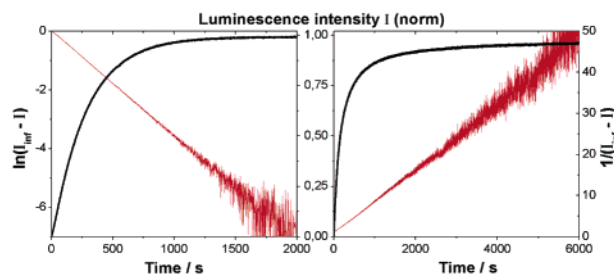


**Figure 2.** Luminescence intensity *I* (black) after mixing of  $\Lambda, \Lambda$ -**B**<sub>4</sub> (left) and  $\Lambda, \Lambda$ -**P**<sub>4</sub> (right) with poly(dA-dT)<sub>2</sub> at 25 °C, [basepair]/[complex] = 8, normalized to 1 at 25 000 s. The logarithmic and inverse scale give rise to linear plots (red), showing that  $\Lambda, \Lambda$ -**B**<sub>4</sub> and  $\Lambda, \Lambda$ -**P**<sub>4</sub> bindings follow first- ( $k_{\text{first}} = 3.4 \times 10^{-3} \text{ s}^{-1}$ ) and second-order ( $k_{\text{second}}[\text{L}]_0 = 7.0 \times 10^{-3} \text{ s}^{-1}$ ) rate laws, respectively.

To account for the different states of the DNA lattice, the kinetics of  $\Lambda, \Lambda$ -**P**<sub>4</sub> threading was modeled by employing the conditional probabilities of a noncooperative McGhee and von Hippel approach.<sup>6</sup> Emission traces were simulated by calculation of the time evolution of the binding density of the threaded (luminescent) complex,  $\theta_D$ , by numerical integration of a rate law comprising two pathways I and II (see Supporting Information).

$$\frac{d\theta_D}{dt} = -\frac{d\theta_B}{dt} = k_I \theta_B (ff)^p + k_{II} \theta_B (ff)^q (fb)$$

where  $\theta_B$  is the binding density of the nonthreaded complex, (*ff*) and (*fb*) are the conditional probabilities that a free binding site is immediately followed by another free binding site and a binding site covered by a nonthreaded complex, respectively. The exponents *p* and *q* are related to the spatial requirements of the transition states of the two pathways I and II (see below). At large [basepair]/[complex] ratios, (*ff*) is close to 1 and (*fb*) is small, yielding pseudo-first-order kinetics through path I. At small ratios, (*ff*) is small and (*fb*), which is roughly proportional to  $\theta_B$ , is relatively large, and

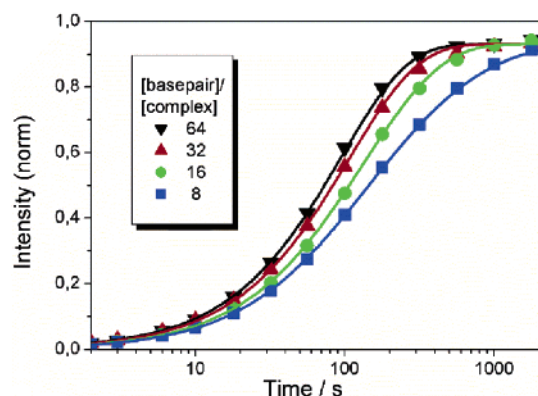


**Figure 3.** Luminescence intensity (symbols) after mixing of  $\Lambda, \Lambda\text{-P}_4$  with poly(dA-dT)<sub>2</sub> at different [basepair]/[complex] ratios (normalized to 1 at 25 000 s). Binding density of intercalated state D (line) obtained from numerical integration of the globally fitted rate law presented in text.

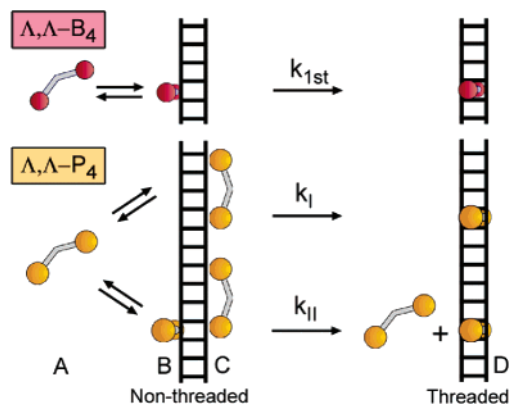


**Figure 4.** Suggested mechanisms for threading intercalation of  $\Lambda, \Lambda\text{-B}_4$  (top) and  $\Lambda, \Lambda\text{-P}_4$  (bottom). From left to right: free complex A in rapid equilibrium with nonthreaded states B (semi-intercalated) and C (groove aligned). The subsequent rearrangement processes give the final threaded state D.

approximate second-order kinetics results via path II. Global fitting to the experimental data at the four mixing ratios gave  $k_I = 12 \times 10^{-3} \text{ s}^{-1}$ ,  $k_{II} = 50 \times 10^{-3} \text{ s}^{-1}$ ,  $p = 11$ , and  $q = 2$ , with an excellent agreement between simulated and measured traces (Figure 3).

Numerous mechanisms might be envisaged that could give rise to the rate expression above. However, an interpretation that also accounts for the kinetics of the  $\Lambda, \Lambda\text{-B}_4$  analogue is schematically presented in Figure 4. Rapid equilibrium exists between free ligand A and two nonthreaded states B and C. The dominating state B is semi-intercalated, while the much less abundant state C is assumed to be aligned along the groove. For  $\Lambda, \Lambda\text{-B}_4$ , the model supposes B to be able to rearrange directly within its basepair pocket to the final threaded state D, whereas the steric hindrance of the larger phenanthroline ligands makes this path unfavorable for  $\Lambda, \Lambda\text{-P}_4$ .

By contrast, the groove-aligned state C allows the middle ring of a phenanthroline ligand of  $\Lambda, \Lambda\text{-P}_4$  to wedge an opening in the base stack. This facilitates the threading through the DNA helix, although it requires a long stretch of free DNA. In the presence of

an adjacent semi-intercalated B state that has partially unstacked the bases, the state C complex is provided an alternative, spatially more efficient mechanism for threading. As a consequence, the threading of  $\Lambda, \Lambda\text{-B}_4$  can be described by a first-order rearrangement independent of binding density, while the requirement a neighboring section of nonthreaded DNA for  $\Lambda, \Lambda\text{-P}_4$  gives rise to a second-order rate law at high binding densities. Assuming the binding site size of the nonthreaded state B ( $n_B$ ) to be 4 basepairs, the results suggest that the binding site size of state C is  $q + n_B = 6$  basepairs and that the transition states of paths I and II involve  $p + n_B = 15$  and  $q + 2n_B = 10$  basepairs, respectively (see Supporting Information). Finally, by assumption, the transition state of  $\Lambda, \Lambda\text{-B}_4$  threading involves  $n_B = 4$  basepairs.

In conclusion, the small structural differences of  $\Lambda, \Lambda\text{-B}_4$  and  $\Lambda, \Lambda\text{-P}_4$  result in large changes in mechanisms for threading intercalation. The  $\Lambda, \Lambda\text{-B}_4$  intercalates into poly(dA-dT)<sub>2</sub> via a simple first-order rearrangement mechanism, as shown by the [basepair]/[complex] independent kinetics. Threading intercalation of the closely related analogue  $\Lambda, \Lambda\text{-P}_4$  to the same polynucleotide is more complex, but can nevertheless be excellently described by numerical integration of a McGhee and von Hippel rate law comprising two separate pathways (see Supporting Information). In contrast to  $\Lambda, \Lambda\text{-B}_4$ , the first-order threading mechanism of  $\Lambda, \Lambda\text{-P}_4$  involves a transition state requiring a long stretch of free DNA. The mechanistic sensitivity to ancillary ligand structures proves the potential of semirigid binuclear ruthenium complexes for selective DNA reactions.

**Supporting Information Available:** Emission traces of  $\Lambda, \Lambda\text{-B}_4$  binding to poly(dA-dT)<sub>2</sub> at the four mixing ratios (Figure S1) and extended explanation of the kinetic analysis. This material is available free of charge via the Internet at <http://pubs.acs.org>.

## References

- (1) (a) Nordén, B.; Lincoln, P.; Åkerman, B.; Tuite, E. *Met. Ions Biol. Syst.* **1996**, *33*, 177–252. (b) Erkkilä, K. E.; Odom, D. T.; Barton, J. K. *Chem. Rev.* **1999**, *99*, 2777–2795. (c) Metcalfe, C.; Thomas, J. A. *Chem. Soc. Rev.* **2003**, *32*, 215–224.
- (2) (a) Friedman, A. E.; Chambron, J. C.; Sauvage, J. P.; Turro, N. J.; Barton, J. K. *J. Am. Chem. Soc.* **1990**, *112*, 4960–4962. (b) Jenkins, Y.; Friedman, A. E.; Turro, N. J.; Barton, J. K. *Biochemistry* **1992**, *31*, 10809–10816. (c) Hiort, C.; Lincoln, P.; Nordén, B. *J. Am. Chem. Soc.* **1993**, *115*, 3448–3454. (d) Haq, I.; Lincoln, P.; Suh, D.; Nordén, B.; Chowdhry, B. Z.; Chaires, J. B. *J. Am. Chem. Soc.* **1995**, *117*, 4788–4796. (e) Lincoln, P.; Broo, A.; Nordén, B. *J. Am. Chem. Soc.* **1996**, *118*, 2644–2653. (f) Lincoln, P.; Tuite, E.; Norden, B. *J. Am. Chem. Soc.* **1997**, *119*, 1454–1455. (g) Lincoln, P.; Nordén, B. *J. Phys. Chem. B* **1998**, *102*, 9583–9594.
- (3) (a) Lincoln, P.; Norden, B. *Chem. Commun.* **1996**, 2145–2146. (b) Wilhelmsson, L. M.; Westerlund, F.; Lincoln, P.; Norden, B. *J. Am. Chem. Soc.* **2002**, *124*, 12092–12093. (c) Wilhelmsson, L. M.; Esbjorner, E. K.; Westerlund, F.; Norden, B.; Lincoln, P. *J. Phys. Chem. B* **2003**, *107*, 11784–11793.
- (4) Önfelt, B.; Lincoln, P.; Nordén, B. *J. Am. Chem. Soc.* **2001**, *123*, 3630–3637.
- (5) At all binding ratios, the concentration of poly(dA-dT)<sub>2</sub> (purchased from Amersham Biosciences) was kept at 120  $\mu\text{M}$  bases. Time-based fluorescence measurements (data collected once every second) were performed in aqueous buffer (150 mM NaCl, 1 mM cacodylate at pH 7.0) on a SPEX fluorolog  $\tau$ -2 spectrofluorometer (JY Horiba) at 25 °C (waterbath controlled).
- (6) (a) McGhee, J. D.; Hippel, P. H. V. *J. Mol. Biol.* **1974**, *86*, 469–489. (b) Lincoln, P. *Chem. Phys. Lett.* **1998**, *288*, 647–656.

JA0521674